INL/JOU-18-52343-Revision-1

Viscosity of 1-Alkyl-1-Methylpyrrolidinium Bis(trifluoromethylsulfonyl)imide Ionic Liquids saturated with Compressed CO2

Ana Rita C. Morais, Mark B. Shiflett, Aaron M. Scurto, Donna L Baek, Robert V Fox, Luis M. Alaras

April 2019

The INL is a U.S. Department of Energy National Laboratory
operated by Battelle Energy Alliance

INL/JOU-18-52343-Revision-1

Viscosity of 1-Alkyl-1-Methylpyrrolidinium Bis(trifluoromethylsulfonyl)imide Ionic Liquids saturated with Compressed CO2

Ana Rita C. Morais, Mark B. Shiflett, Aaron M. Scurto, Donna L Baek, Robert V Fox, Luis M. Alaras

April 2019

Idaho National Laboratory
Idaho Falls, Idaho 83415

http://www.inl.gov

Prepared for the
U.S. Department of Energy
Office of Nuclear Energy
Under DOE Idaho Operations Office
Contract DE-AC07-05ID14517

Revision Submitted to Journal of Chemical & Engineering Data: February 19th, 2019

Viscosity of 1-Alkyl-1-Methyl-Pyrrolidinium Bis(trifluoromethylsulfonyl)imide Ionic Liquids saturated with Compressed CO_2

Ana Rita C. Morais[†], Luis M. Alaras[†], Donna L. Baek[∝], Robert V. Fox[∝], Mark B. Shiflett[†‡] and Aaron M. Scurto[†]*

[†] Department of Chemical & Petroleum Engineering and Center for Environmentally Beneficial Catalysis, University of Kansas, Lawrence, Kansas 66045, United States.

[∝] Idaho National Laboratory, Idaho Falls, ID 83415, United States.

* Corresponding author, Aaron M. Scurto, ascurto@ku.edu

Abstract

The viscosity of mixtures of pyrrolidinium-based ionic liquids saturated with compressed CO_2 was measured using a high-pressure viscometer at three different temperatures (298.15, 318.15 and 338.15 K). The high-pressure viscosity of 1-propyl-1-methyl-pyrrolidinium ([C_3C_1pyr]), 1-butyl-1-methyl-pyrrolidinium ([C_4C_1pyr]), and 1-hexyl-1-methyl-pyrrolidinium bis(trifluoromethylsulfonyl)imide ([C_6C_1pyr]) cations with common anion, bis(trifluoromethylsulfonyl)imide ([NTf_2]), was measured up to a maximum CO_2 pressure of 25 MPa. This viscosity ranged from 3.3 to 98.3 mPa.s. The viscosity of the ionic liquid/ CO_2 mixture dramatically decreases with increasing of CO_2 pressure up to approximately 7 MPa beyond which the viscosity decrease becomes more marginal. This is due to the vapor-liquid equilibrium (CO_2 solubility) of the IL/CO_2 system. The viscosity decrease at lower temperatures is more significant due to the higher CO2 solubility. The effect of alkyl chain length of the cation on the viscosity of ionic liquid/ CO_2 mixture was also measured. Though the pure [$C_nC_1$pyr][NTf_2] viscosity increases significantly with the increasing alkyl chain length of the cation, the viscosity of the ionic liquid/CO_2 mixtures become quite similar at higher CO_2 pressures (composition).

Keywords: Compressed carbon dioxide, Cation effects, High-pressure viscosity, Pyrrolidinium ionic liquids.

1. Introduction

Room-temperature ionic liquids (RTILs) are a class of organic salts with unique properties. They have negligible vapor pressure, tunable solubility and generally good thermal stability. These low-melting salts, which are composed of an organic cation (such as imidazolium, pyrrolidinium, pyridinium, etc.) and an organic or inorganic anion (such as bis(trifluoromethylsulfonyl)imide, dicyanimide, etc.), can be designed molecularly for advantageous thermodynamic properties, transport properties, chemical properties, etc.[1] A judicious selection of cations, anions, and substituents can yield ILs with relatively low ambient viscosity. This is one of the main reason for the popularity of ionic liquids containing bis(trifluoromethylsulfonyl)imide [NTf_2] anion.[2, 3] In the light of these considerations, the versatility of ionic liquids as replacements of conventional volatile organic solvents in a number of specific applications, *e.g.* in liquid-liquid separations,[4, 5] electrochemical applications,[6-8] chemical reactions,[9-11] multiphase bioprocess operations[12, 13] and CO_2 capture[14, 15] has been intensively investigated.

Mixtures of ionic liquid and CO_2 are of particular interest because CO_2 has a remarkably high solubility in the ionic liquid, whereas ionic liquid is not soluble in the CO_2 phase even at high pressures. This unique behavior offers a highly attractive approach for the development of more sustainable and economically homogeneous and heterogeneous catalyzed processes.[16, 17] The development of these ionic liquid+CO_2-based systems requires essential thermodynamic properties, of which a number of studies have been done on phase behavior and solubility.[18-23] However, detailed knowledge on the transport properties, such as viscosity, thermal conductivity, and diffusivity, of mixtures of ionic liquids with CO_2 is still rather scarce. These properties are very important in the design and implementation of any industrial process.

Many research groups have measured the viscosity of pure ionic liquids at various temperatures and pressures. Recently, Yadav *et al.* have measured the viscosity of a series of ionic liquids to assess the influence of the nature of cation and anion in a temperature range from 283.15 to 363.15 K.[24] Ahosseini and Scurto measured the pressure effect on viscosity of pure 1-alkyl-3-methyl-imidazolium-based ionic liquids with various alkyl-chain lengths and anions up to 126 MPa and 343.15 K temperature using an oscillating-piston viscometer.[25] In one of the first investigations of viscosity of IL/CO_2 mixtures, Lu *et al.* determine the micro-viscosity of 1-butyl-3-methyl-imidazolium hexafluorophosphate [BMIm][PF_6] with CO_2 mixtures using a spectroscopic probe.[26] Liu *et al.* investigated the effect of high-pressure CO_2 on the viscosity of mixtures of 1-butyl-3-methyl-imidazolium hexafluorophosphate [BMIm][PF_6] and methanol with a falling ball viscometer.[27] Tomida *et al.* measured the viscosities of [BMIm][PF_6] and [BMIm][BF_4] + CO_2 mixtures at temperature range from 293.15 to 353.15 K and pressures up to 20 MPa.[28, 29] Scurto and coworkers measured the viscosity of a variety of 1-alkyl-3-methyl-imidazolium bis(trifluoromethylsulfonyl)imide ionic liquids saturated with compressed CO_2 using an oscillating-piston viscometer.[30] More recently, Lopes *et al.* measured the viscosity of CO_2 saturated 1-allyl-3-methylimidazolium chloride.[31] Smith and coworkers measured the viscosity of ionic liquid/cellulose mixture under compressed CO_2 conditions.[32] In most of these studies, an accentuated drop in liquid viscosity of ionic liquid occurs with CO_2 pressure (composition). In contrast to previous reports, Goodrich *et al.* showed that the addition of CO_2 to amine-functionalized anion-tethered ionic liquids (*e.g.*, trihexyl(tetradecyl)phosphonium glycinate [P_{66614}][Gly]) resulted in a dramatic increase on viscosity. However, the chemical absorption of CO_2 in [P_{66614}][Gly] versus physical absorption in other reports, likely due to the formation of hydrogen bonding network, seems to be the main reason for the increased viscosity in this system. [33]

1.1. Scope and Objectives of the study

In the present work, we measure the liquid dynamic viscosity (η) of three 1-n-alkyl-1-methyl -pyrrolidinium bis(trifluoromethylsulfonyl)imide ionic liquids (Figure 1) saturated with CO_2 as a function of temperature (298.15, 318.15, and 338.15 K) and CO_2 pressure (up to 250 bar). The effect of alkyl-chain length is also investigated for 1-ethyl- (n=1 in Figure 1), 1-propyl- (n=2), and 1-n-hexyl-3-methylpyrrolidinium (n=5) cations. Concurrent with these studies, we have recently measured the vapor-liquid equilibrium thermodynamics with the same ionic liquids and CO_2[34] to determine the liquid phase CO_2 composition at the temperatures and pressures of interest in this study.

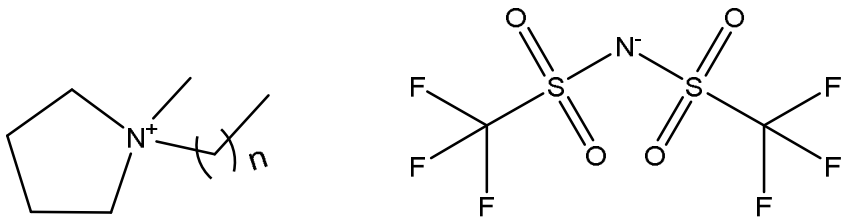

1-n-alkyl-1-methyl pyrrolidinium bis(trifluoromethylsulfonyl)imide

Figure 1. Chemical structures of the 1-n-alkyl-1-methyl-pyrrolidinium bis(trifluoromethylsulfonyl)imide ionic liquids investigated in the present work.

2. Experimental section

2.1. Materials

Research grade carbon dioxide (99.999% purity, LOT# 9106205709A4) was purchased from Matheson Tri-Gas and used as received. 1-propyl-1-methyl-pyrrolidinium bis(trifluoromethylsulfonyl)imide $[C_3C_1pyr][NTf_2]$, 1-butyl-1-methyl-pyrrolidinium bis(trifluoromethylsulfonyl)imide $[C_4C_1pyr][NTf_2]$, and 1-hexy-l-methyl-pyrrolidinium bis(trifluoromethylsulfonyl)imide $[C_6C_1pyr][NTf_2]$ were obtained from IoLiTec Ionic Liquid Technologies and dried under vacuum at approximately 10^{-5} MPa, 348.15 K for 24 h. Water content was measured upon delivery using a Mettler Toledo DL36 Coulometric Karl Fisher

titrator. Manufacturer ionic liquid specifications, purities, and water content measured are listed in Table 1.

Table 1. Specifications, purities, and water content of the chemicals used in this work.

Chemicals	Abbreviation	Source	CAS number	Purity/ %	Water content/ ppm
Carbon dioxide	CO_2	Matheson Tri-Gas, Inc	124-38-9	99.99	N/A
1-propyl-1-methyl-pyrrolidinium bis(trifluoromethylsulfonyl)imide	$[C_3C_1pyr][NTf_2]$	Iolitec	223437-05-6	>99.5	38±3
1-butyl-1-methyl-pyrrolidinium bis(trifluoromethylsulfonyl)imide	$[C_4C_1pyr][NTf_2]$	Iolitec	223437-11-4	>99.5	110±1
1-hexyl-1-methyl-pyrrolidinium bis(trifluoromethylsulfonyl)imide	$[C_6C_1pyr][NTf_2]$	Iolitec	380497-19-8	>99.5	23±2

2.2. High-Pressure Viscosity Measurements

The high-pressure viscosity of the ionic liquid and CO_2 mixtures were measured with a modified Cambridge Applied Systems (currently Cambridge Viscosity-PAC) high-pressure viscometer (ViscoPVT/ViscoPro 2000 System 4-SPL-440). The apparatus and measurement procedure has been described in detail in a prior reference; however, a brief overview will be given herein. A high-pressure equilibrium Jerguson view cell was used to mix the ionic liquids with CO_2. A recirculation pump was used to draw the ionic liquid saturated with CO_2 from the view cell through the viscosity measurement sensor, and then back to the view cell. Thus, mixing the liquid with the gas phase providing convection to both the interface and inside each phase. After thermodynamic equilibrium was achieved (varies between 20 to 60 min for high CO_2 compositions (low viscosity) and low compositions (high viscosity),

respectively, at high recirculation rates) the recirculation pump was stopped and the mixture containing ionic liquid and CO_2 was isolated for the measurement inside of the viscometer. For higher CO_2 pressure, the process was repeated. The viscosity measurement device is based on the movement of a piston (rod) inside of the cylindrical chamber producing annular flow. Two magnetic coils inside the body of the sensor oscillate the piston over a fixed distance, forcing the fluid to flow through the annular space between the rod and chamber. The time required for the rod to complete a round trip is directly related to the viscosity of the fluid. The viscometer sensor is capable to measuring viscosity from 0.2 to 10,000 cP (mPa·s), in a temperature range of 233.15 to 383.15 K.

2.3. Uncertainty

The viscosity reading is the average of 10 measurements with the respective standard deviations used as the uncertainty at each point. The inherent uncertainty in the viscometer has been estimated rigorously elsewhere[25, 35] and is generally less that ± 1.0%: usually less than the random error reported as the standard deviations. The nominal uncertainty of the pressure gauge is 0.07% full-scale (FS = 206.8 MPa); but the National Institute of Standards and Technology (NIST)-traceable calibration was accurate to 0.0084% full-scale. The maximum temperature fluctuation from the reported set-point temperature for all results was less than 0.2 K.

3. Results and Discussion

3.1. Pure $[C_nC_1pyr][NTf_2]$ viscosity measurements and comparison with literature data

The ambient-pressure viscosity (of three ionic liquids, 1-propyl-1-methyl-pyrrolidinium ($[C_3C_1pyr]$), 1-butyl-1-methyl-pyrrolidinium ($[C_4C_1pyr]$), and 1-hexyl-1-methyl-

pyrrolidinium ([C_4C_1pyr]) cations with bis(trifluoromethylsulfonyl)imide ([NTf_2]) anion were obtained as function of temperature from 298.15 to 338.15 K. The viscosity of pure ionic liquids with temperature was compared with reported literature data and listed in Table 2. A comparison of experimental viscosity obtained with all the data presented in the literature allowed for making not only general qualitative conclusions on validation of our data with the literature ones but also on general trends. In general, the obtained data are in good agreement with the previous reports.[36-42] For instance, the viscosities of all of our data [$Pyr_{1,R}$][Tf_2N] are within 1.1% AARD ($\%AARD = \frac{100}{N}\sum_{J-1}^{N}\left|\frac{\eta_j^{here}-\eta_j^{lit}}{\eta_j^{lit}}\right|$) of those reported by Jin *et al.*[36] at the same temperatures as our study for all three ILs. The comparison of obtained results with a wide variety of data sources for [C_3C_1pyr][NTf_2], [C_4C_1pyr][NTf_2] and [C_6C_1pyr][NTf_2] allowed us to confirm the veracity of the experimental technique at ambient pressure. In addition, the viscosities found for [C_3C_1pyr][NTf_2], [C_4C_1pyr][NTf_2] and [C_6C_1pyr][NTf_2] even at low temperature (*e.g.* 298.15 K) are suitable for industrial applications, because all of the ILs have viscosities comparable (< 100 mPa.s) to those found in organic solvents (0.2-100 mPa.s).[43]

Considering the strong dependence of viscosity on water content, it is important to point out that in certain cases the discrepancies between literature data could be attributed to slight differences in water content. The observed influence of alkyl chain length on viscosity is generally consistent with the information available in the literature. For instance, when comparing the viscosities of different ionic liquids at 298.15 K, it is clear that the increase on the length of the alkyl chain of the cation increases the viscosity, as shown by comparing [C_3C_1pyr][NTf_2], [C_4C_1pyr][NTf_2] and [C_6C_1pyr][Tf_2N]. This increase in the viscosity with increasing alkyl chain length on the cation is in agreement with the reports on pyrrolidinium- and phosphonium-based ionic liquids.[33, 36] This is also similar to the qualitative trend for 1-n-

alkyl-3-methylimidazolium [Tf_2N] ionic liquids, where increasing chain length from ethyl to n-hexyl increases the viscosity at a given temperature (and pressure).[25] As depicted in Table 2, in the temperature range studied, the viscosity considerably decreased with increasing temperature. It is most striking for [C_3C_1pyr][NTf_2], which has a 4.5-fold reduction in viscosity at 338.15 K than at 298.15 K. At 298.15 K, great differences in the results obtained for the investigated ionic liquids were found (from 98.3 for [C_6C_1pyr][NTf_2]) to 56.6 mPa·s for [C_3C_1pyr][NTf_2], while all the ionic liquids studied tend to have closer viscosities at 338 K. Thus, temperature has a much greater influence on the viscosity than the length of alkyl chain of the cation between ethyl- and n-hexyl groups.

Table 2. Experimental dynamic viscosity (η) of $[C_3C_1pyr][NTf_2]$, $[C_4C_1pyr][Tf_2N]$ and $[C_6C_1pyr][NTf_2]$ as function of temperature at ambient pressure, and comparison with the literature data.

Ionic liquid	T (K)	Experimental (η) (mPa·s)	(η) reported in literature (mPa·s)
$[C_3C_1Pyr][NTf_2]$	298.15	56.6 ± 0.5	54.4;[36] 63;[41] 49.4;[40] 61.5.[42a]
	318.15	26.5 ± 0.1	27.0;[36] 22.4;[40] 29.2.[42a]
	338.15	15.6 ± 0.1	15.6;[36] 13.4;[40] 16.4.[42a]
$[C_4C_1Pyr][NTf_2]$	298.15	75.6 ± 0.2	75.7;[36] 81.4;[40] 76.7;[37] 77.6;[38] 77.8;[39a] 79.6;[44] 75.9;[45] 76.9;[46] 77.3.[47]
	318.15	34.3 ± 0.1	34.5;[36] 34.7;[40] 34.7;[37] 34.8;[38] 34.8;[39a] 35.6;[44] 33.5;[45] 34.3;[46] 34.7.[47]
	338.15	18.6 ± 0.1	18.7;[36] 18.7;[40] 19.2;[37] 18.8;[38] 18.8;[39a] 19.2;[44] 17.8;[45] 18.4;[46] 17.8.[47]
$[C_6C_1Pyr][NTf_2]$	298.15	98.3 ± 0.1	96.6[36]
	318.15	41.4 ± 0.0	42.0[36]
	338.15	21.9 ± 0.0	22.1[36]

Standard Uncertainties: u(T)=0.1 K; u(P)=0.05 bar; u(η)=0.5 mPa·s. [a] Viscosity value was estimated from the interpolation of the reported data at the desired temperature.

3.2. Viscosity of CO_2-saturated $[Pyr_{1,R}][Tf_2N]$ ionic liquids

3.2.1. $[C_3C_1Pyr][NTf_2]$/ CO_2 mixtures

The $[C_3C_1Pyr][NTf_2]$ + CO_2 mixture viscosities were measured for pressures up to approximately 25 MPa and three different isotherms at 298.15, 318.15 and 338.15 K.

Table **3** depicts the measured dynamic viscosity (η), interpolated density (ρ) and calculated kinematic viscosity of the $[C_3C_1Pyr][NTf_2]$ as function of CO_2 pressure and composition. The effect of pressure on the liquid dynamic viscosity of CO_2-saturated $[C_3C_1Pyr][NTf_2]$ and on CO_2 solubility at 318.15 K is illustrated in Figure 2. The temperatures of 318.15 and 338.15 K are above of critical temperature of pure CO_2 (304.25 K) and, thus, there is a continuous vapor-liquid equilibrium curve from low to high pressures. As shown, the viscosity decreased considerably with the increase of CO_2 pressure to approximately 7 MPa and 318.15 K. At this pressure, the mixture viscosity was approximately 80 % lower than of the pure ionic liquid viscosity (at ambient pressure). After approximately 7 MPa of CO_2 pressure, the viscosity reduction became less significant with the increase of CO_2 pressure. For instance, a viscosity decrease of only 30% was found with an increase of CO_2 pressure from 7 to 25 MPa. Similar results were obtained by Lu *et al.* who found that the micro-viscosity of $[C_4C_1im][PF_6]$ is 6.5-fold reduced as the CO_2 pressures increased from 0 (without CO_2) to 6.8 MPa at 308.15 K.[48] However, this is not a pressure effect as the viscosity of the pure IL negligibly increased in the pressure range investigated.[25] Instead, the increase in liquid CO_2 composition resulted in a large increase of CO_2 solubility in the ionic liquid for pressures ranging from 0.1 to 7 MPa.

We have recently measured the high-pressure vapor-liquid equilibrium (VLE) of the ionic liquids studied here with CO_2.[34] This data allowed us to interpolate the CO_2 compositions of the liquid-phase at the experimental temperature and pressures of the viscosity measurements. The secondary y-axis of Figure 2 illustrates the solubility of CO_2 in the ionic liquid. The viscosity behavior is nearly the mirror image of the solubility results indicating the proportionality. Dissolving low-viscosity CO_2 dramatically improves the momentum transport properties of the ionic liquid. In the light of these observations, significant advantages of ionic liquid/CO_2 mixtures as a replacement of conventional volatile organic solvents for reactions and separations are highlighted.

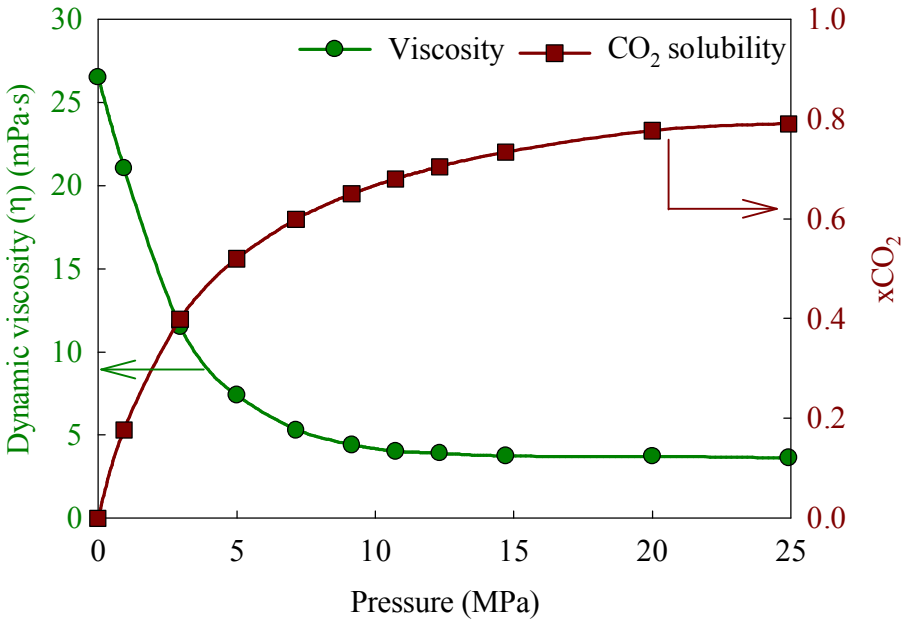

Figure 2. Effect of CO_2 pressure on liquid viscosity and on mole fraction concentration of CO_2 in $[C_3C_1Pyr][NTf_2]$ at 318.15 K (smoothed lines). Solubility data is interpolated from Ref. [34]. The lowest pressure viscosity point is free of CO_2 at ambient pressure.

Table 3. Measured dynamic viscosity (η), interpolated density (ρ) and calculated kinematic viscosity (ν) of the $[C_3C_1Pyr][NTf_2]$ phase with respect to CO_2 pressure and composition.

T (K)	p (MPa)	x_{CO2} [a]	η (mPa·s)	± [b]	ρ ($g \cdot cm^{-3}$) [c]	ν (cSt) [d]	± [e]
298.15	-	0	56.6	0.5	1.427	40	4
298.15	1.96	0.388	27.7	0.1	1.422	19.5	0.1
298.15	3.12	0.518	17.28	0.09	1.414	12.23	0.09
298.15	4.03	0.594	11.13	0.02	1.405	7.92	0.04
298.15	5.03	0.660	8.62	0.03	1.394	6.18	0.04
298.15	6.00	0.711	6.78	0.04	1.382	4.91	0.04
298.15	6.40 [f]	0.729	6.07	0.03	1.376	4.41	0.03
298.15	9.76 [g]	0.781	5.43	0.03	1.354	4.01	0.03
298.15	6.43 [h]	1.0	0.057 [h]	-	0.7105 [h]	0.0803 [h]	-
318.15	-	0	26.48	0.08	1.409	18.8	0.1
318.15	0.93	0.178	21.04	0.06	1.446	14.55	0.08
318.15	2.96	0.400	11.50	0.03	1.423	8.09	0.05
318.15	5.00	0.521	7.38	0.01	1.393	5.30	0.03
318.15	7.14	0.600	5.29	0.02	1.355	3.91	0.02
318.15	9.15	0.651	4.40	0.02	1.355	3.25	0.02
318.15	10.73	0.681	4.02	0.02	1.354	2.97	0.02
318.15	12.32	0.705	3.90	0.03	1.354	2.88	0.02
318.15	14.71	0.734	3.74	0.03	1.353	2.76	0.03
318.15	20.01	0.777	3.71	0.03	1.353	2.74	0.03
318.15	24.92	0.791	3.62	0.04	1.351	2.68	0.03
338.15	-	0	15.55	0.05	1.392	11.18	0.07
338.15	2.01	0.252	10.55	0.03	1.392	7.58	0.04
338.15	3.01	0.341	8.83	0.03	1.397	6.32	0.04
338.15	4.06	0.417	7.55	0.01	1.405	5.37	0.03
338.15	5.10	0.479	6.47	0.03	1.414	4.58	0.03
338.15	6.00	0.526	5.90	0.02	1.423	4.14	0.03
338.15	7.52	0.592	5.00	0.03	1.439	3.38	0.03
338.15	10.10	0.676	4.05	0.03	1.461	2.67	0.02
338.15	12.51	0.735	3.63	0.03	1.470	2.46	0.02
338.15	14.91	0.781	3.37	0.03	1.459	2.30	0.02

Standard Uncertainties: u(T)=0.1 K; u(p)=0.1MPa; u(ρ)=0.001g·cm^{-3}; u(η)=0.1mPa·s u(ν)=0.5 cSt. [a] Compositions were determined by interpolation of the VLE data of Ref. [34]. [b] standard deviation of 20 measurements; [c] interpolated from density data of Ref. [34]; [d] kinematic viscosity (ν) is defined as: $\nu = \frac{\eta}{\rho}$, where η is the dynamic viscosity and ρ is the mixture density ; [e] assumes a 5% error in the interpolated molar volume; [f] Vapor-Liquid-Liquid Equilibrium point: IL-rich phase viscosity; [g] Liquid-Liquid Equilibrium point: IL-rich phase; [h] properties of pure saturated liquid CO_2 from Ref. [49].

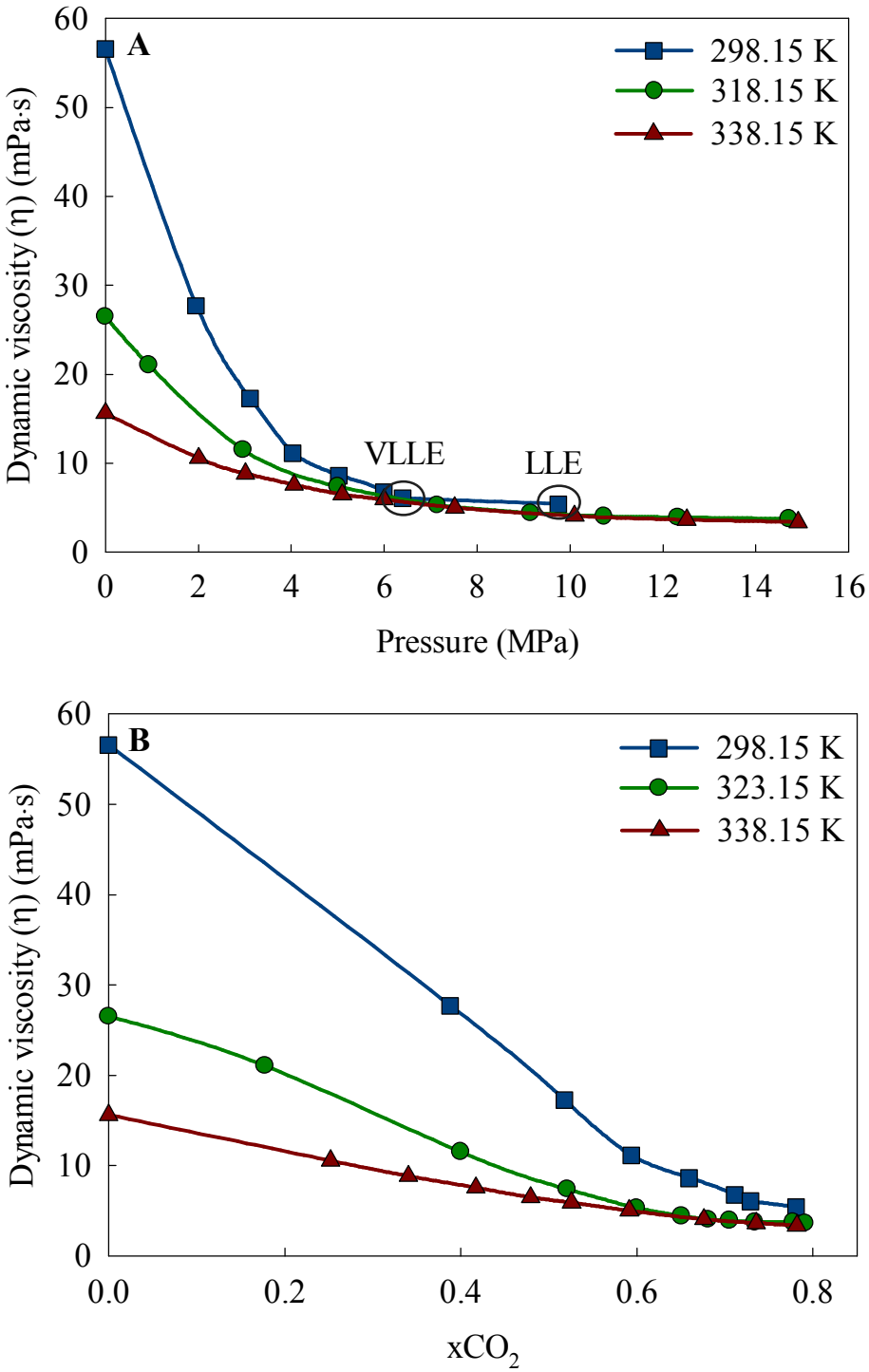

Figure 3. The viscosity of CO_2-saturated $[C_3C_1Pyr][NTf_2]$ as a function of CO_2 pressure (A) and mole fraction concentration of CO_2 in the liquid phase (B) at 298.15, 318.15 and 338.15 K isotherms (smoothed lines). The lowest pressure/ composition viscosity point is free of CO_2 at ambient pressure.

Figure 3 depicts the influence of CO_2 pressure (Figure 3A) and the CO_2 composition (Figure 3B) in the liquid phase on the viscosity for the three isotherms. In contrast to the plot at 318.15K (Figure 2), for temperatures below CO_2 critical temperature, *e.g.* 298.15 K, vapor-liquid equilibrium transitions to vapor-liquid-liquid (VLLE) (experimentally confirmed) near the vapor pressure of the pure CO_2 with an IL-rich liquid in equilibrium with a CO_2-rich liquid in equilibrium with a CO_2-rich vapor phase. Above the vapor pressure (64.3 bar at 298.15K), the system becomes liquid-liquid equilibrium (LLE) with an IL-rich liquid in equilibrium with a CO_2-rich liquid. This CO_2-rich liquid and vapor phases in both VLLE and LLE are pure CO_2 (or nearly pure down to the ppm level) as pointed out in the literature.[50] In either situation, only the viscosity of the IL-rich liquid phase is reported.

The decrease in viscosity of CO_2-saturated $[C_3C_1Pyr][NTf_2]$ showed a general trend with respect to the CO_2 composition in the liquid phase and CO_2 pressure for all temperatures studied herein. In pure $[C_3C_1Pyr][NTf_2]$ (at ambient pressure), the effect of temperature on the viscosity was significant; however, these viscosity differences become smaller as the CO_2 pressure increases. For instance, there was only a small viscosity difference between the various isotherms generated by this study as the CO_2 pressure was greater than about 7 MPa (Figure 3A). Also, the viscosity of the $[C_3C_1Pyr][NTf_2]$ decreases dramatically with increasing CO_2 pressure, up to 5 MPa, where the viscosity reduction as a function of CO_2 pressure became less evident. These data indicate that for the lower CO_2 pressures, the solubility of CO_2 in the ionic liquid varies more significantly with the temperature and therefore, the temperature plays a major role on the viscosity decrease. Conversely, at greater CO_2 pressures, the CO_2 mole fraction for various temperatures are very similar, which makes the variation in viscosity less sensitive with temperature. Thus, the dissolution of CO_2 can attenuate the role of temperature on reducing the viscosity of the ionic liquid. Similar findings were obtained by Liu *et al.* and Tomida *et al.*, who investigated the effect of CO_2 pressure on

the viscosity of $[C_4C_1im][PF_6]$ at various temperatures.[27, 28] They demonstrated that the viscosity of liquid phase decreases with increasing CO_2 pressure and the influence of temperature is not noticeable at high CO_2 pressures. However, comparing the viscosity of the $[C_3C_1Pyr][NTf_2]$ at 298.15 K with either 318.15 or 338.15 K, allowed us to conclude that the differences in the viscosities are still beyond experimental uncertainty of our measurements even at higher CO_2 mole fraction. In the light of these observations, the effect of temperature on reducing the viscosity of the ionic liquid could not be completely overcome by CO_2 dissolution when comparing 298.15 K with either 318.15 or 338.15 K.

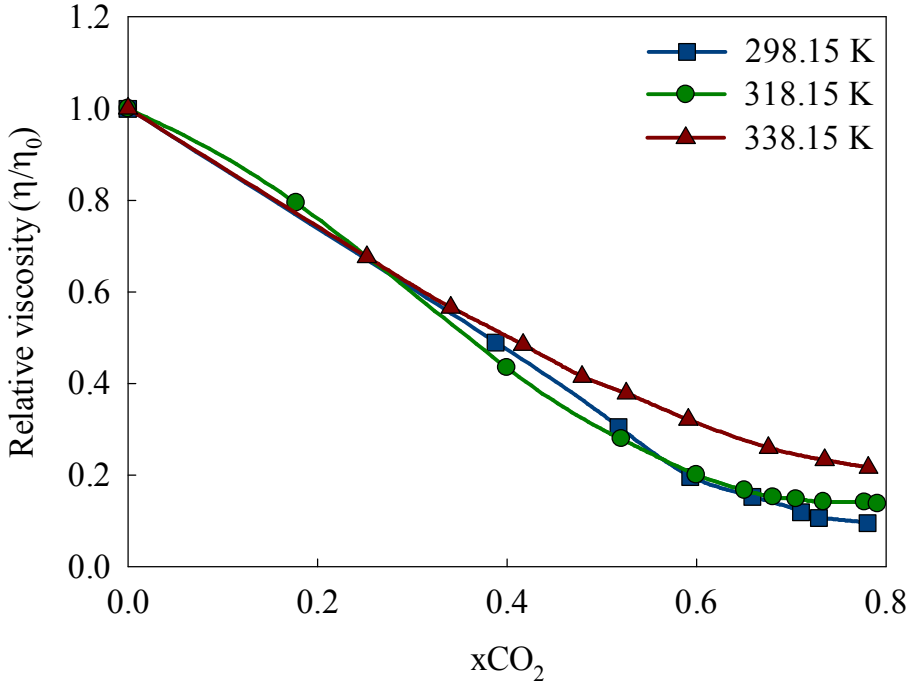

Figure 4. Normalized viscosity to the ambient pressure viscosity of pure $[C_3C_1Pyr][NTf_2]$ as function of CO_2 composition at 298.15, 318.15 and 338.15 K isotherms (smoothed lines). The lowest composition/ viscosity point is free of CO_2 at ambient pressure.

Compressed CO_2 reduces the viscosity of the ionic liquid solutions, which can increase or improve the mass transfer and heat transfer properties of the IL solution. This may in turn improve catalytic reactions and extraction processes relative to pure ionic liquid. Interestingly, when viscosities are normalized (mixture viscosity (η) divided by pure ionic

liquid viscosity at ambient pressure (η_0) at the temperature of interest), the relative viscosity of the $[C_3C_1Pyr][NTf_2]$ with increasing of CO_2 mole fraction is linear and nearly identical amongst the three isotherms for the lower CO_2 mole fractions, as shown in Figure 4. However, at greater CO_2 compositions (CO_2 mole fraction > 0.30), the viscosity differences between 338.15 K and the remaining temperatures studied started to increase significantly. This suggests that the CO_2 composition in the ionic liquid is the major factor contributing to the observed viscosity reduction. The variation of liquid density is not very pronounced with CO_2 mole fraction, as shown in

Table **3**. As depicted in Figure 5, the kinematic viscosity has very similar qualitative trends as the dynamic viscosity, including temperature and CO_2 composition effects.

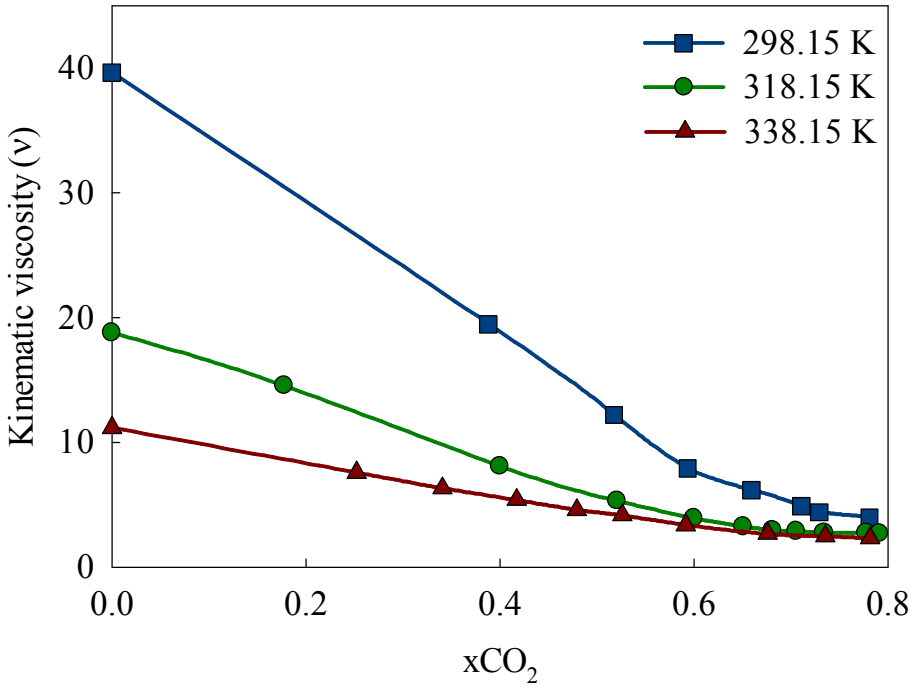

Figure 5. Kinematic viscosity (ν) of $[C_3C_1Pyr][NTf_2]$ as function of CO_2 composition at 298.15, 318.15 and 338.15 K isotherms (smoothed lines). The lowest composition viscosity point is free of CO_2 at ambient pressure.

3.2.2. $[C_4C_1Pyr][NTf_2]$/ CO_2 and $[C_6C_1Pyr][NTf_2]$/ CO_2 mixtures

To assess the influence of the alkyl-group linked to pyrrolidinium ring on the CO_2-saturated viscosity, measurements were conducted for long-chain $[C_4C_1Pyr][NTf_2]$ and $[C_6C_1Pyr][NTf_2]$ ionic liquids at 298.15, 318.15 and 338.15 K and various CO_2 pressures.

Table **4** and

Table **5** list the measured dynamic viscosity (η), interpolated density (ρ) and calculated kinematic viscosity (ν) of $[C_4C_1Pyr][NTf_2]$ and $[C_6C_1Pyr][NTf_2]$ as function of pressure and composition of CO_2. In addition,

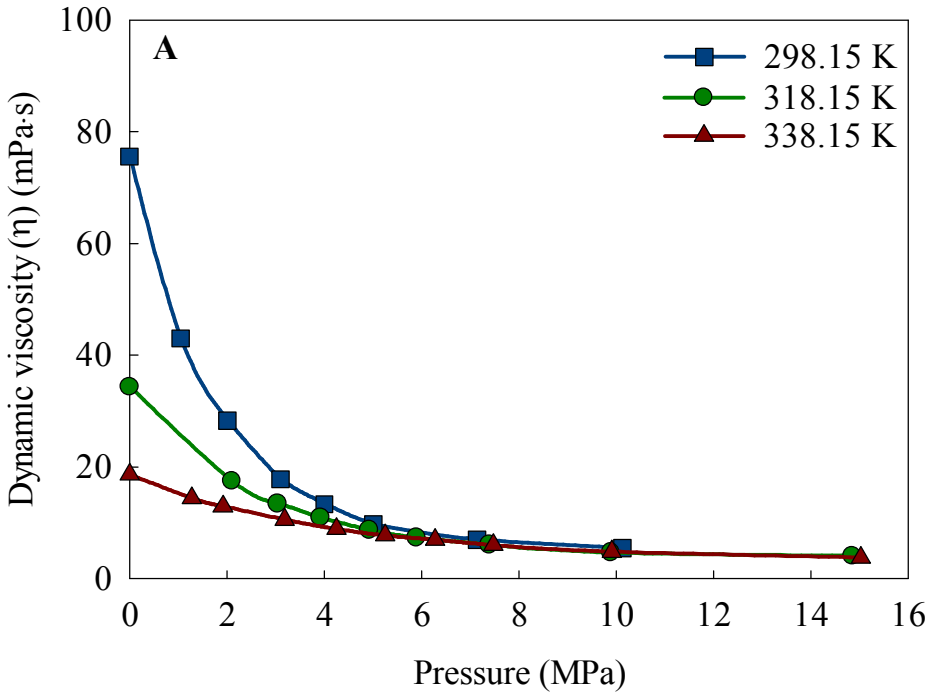

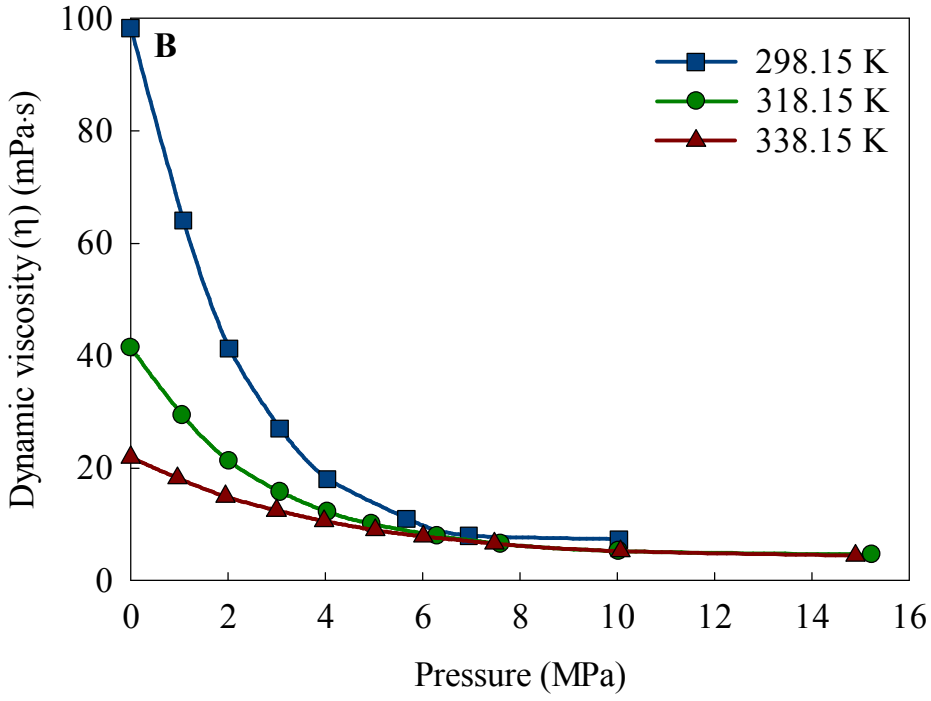

Figure 6 illustrates the effects of CO_2 pressure and temperature on the viscosity of

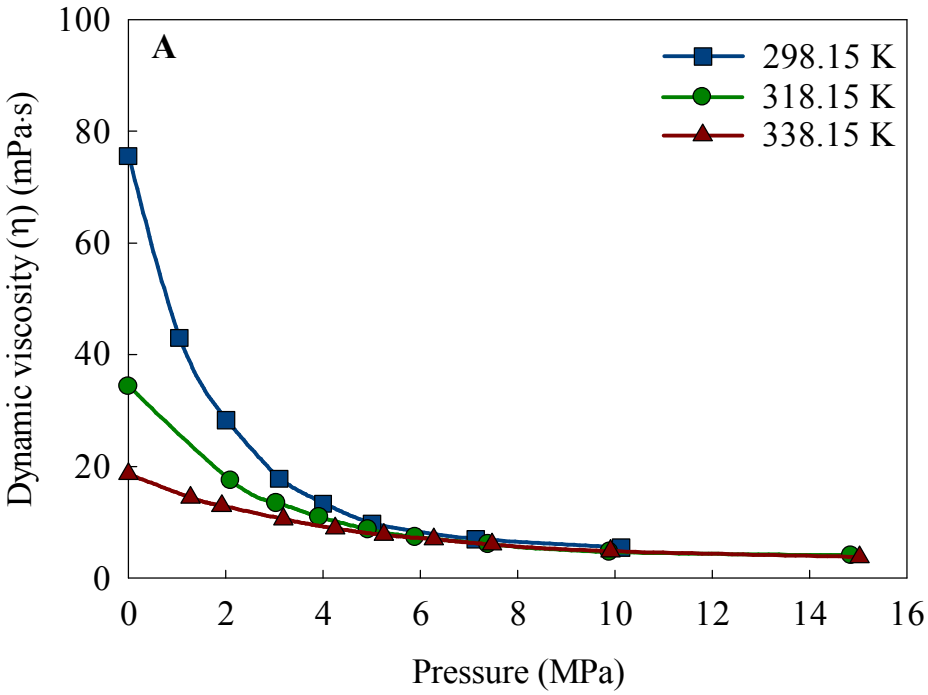

$[C_4C_1Pyr][NTf_2]$ (

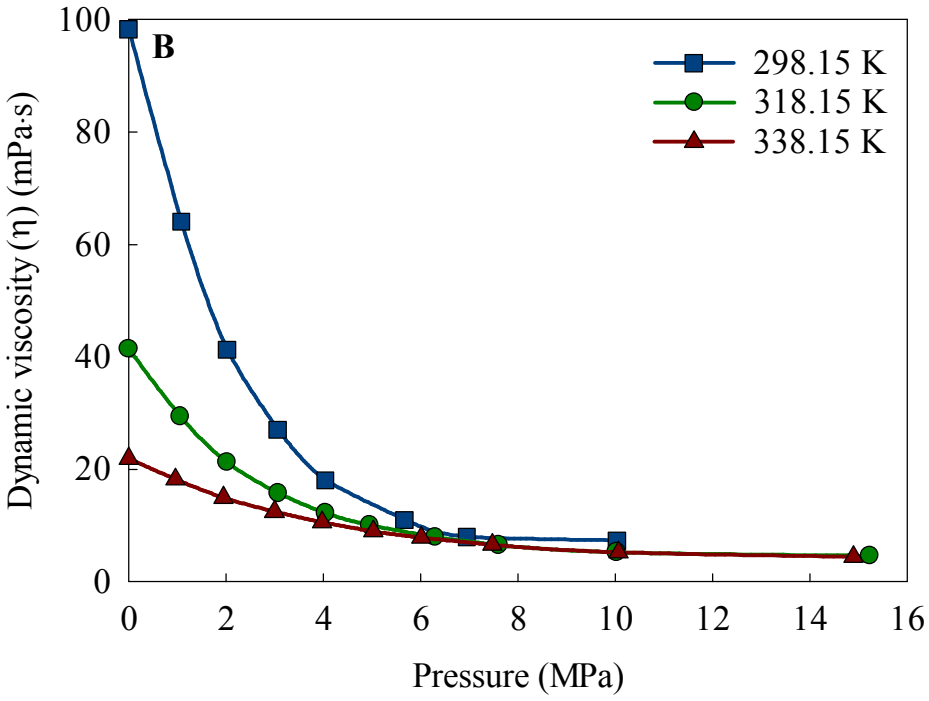

Figure 6A) and [C_6C_1Pyr][NTf_2] (

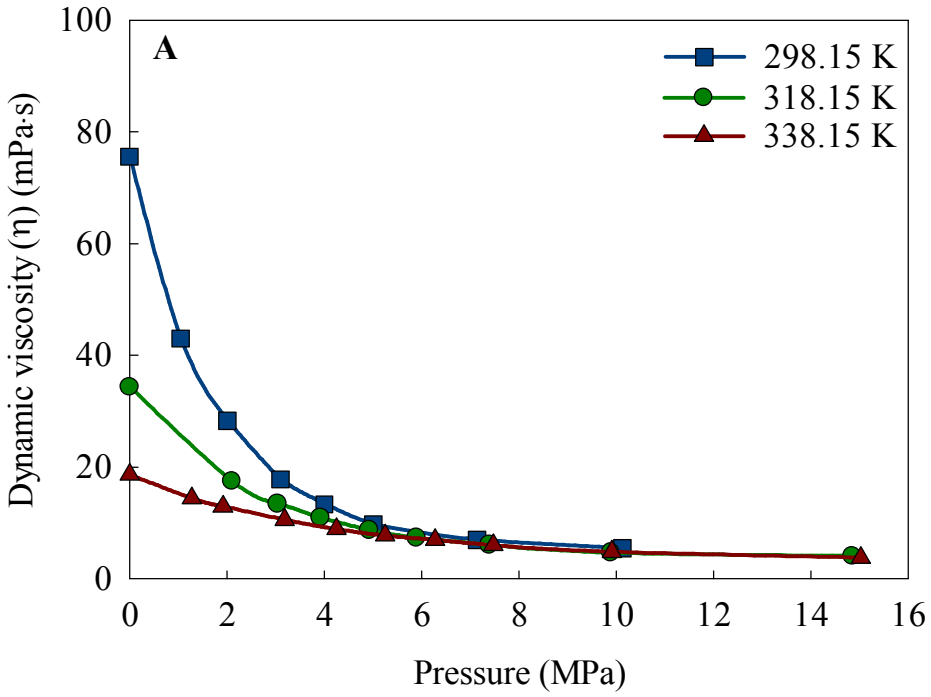

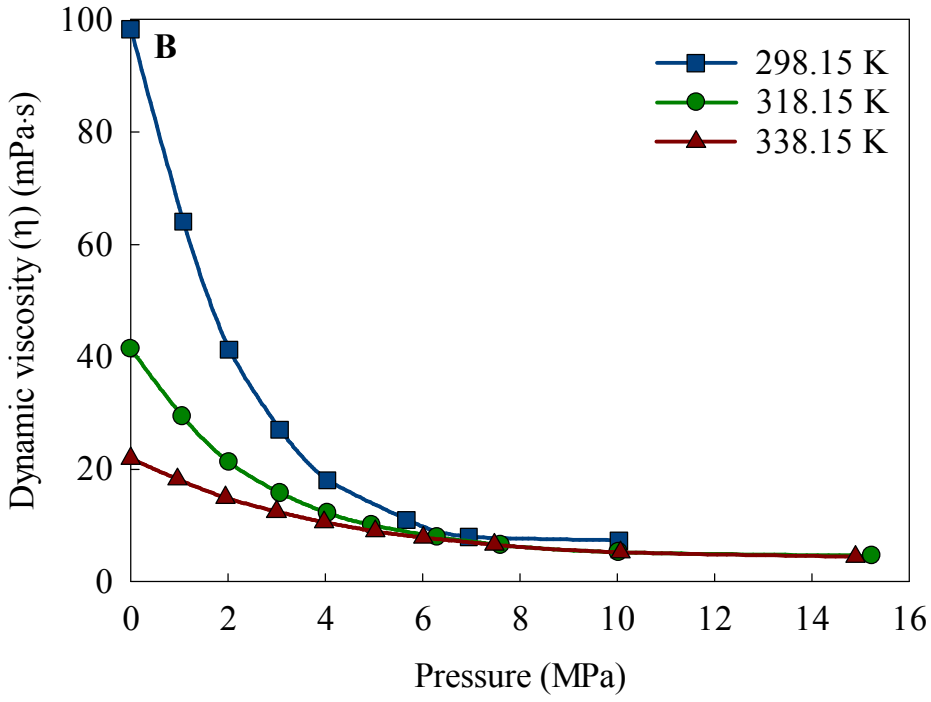

Figure 6B). The qualitative trends for each ionic liquid is similar to that of [C_3C_1Pyr][NTf_2], as the solubility of CO_2 in [C_4C_1Pyr][NTf_2] and [C_6C_1Pyr][NTf_2] is very similar to what has been found for [C_3C_1Pyr][NTf_2].

Table 4. Measured dynamic viscosity (η), interpolated density (ρ) and calculated kinematic viscosity (ν) of the $[C_4C_1Pyr][NTf_2]$ phase with pressure and composition of CO_2.

T (K)	p (MPa)	xCO_2 [a]	η (mPa·s)	± [b]	ρ (g·cm^{-3}) [c]	ν (cSt) [d]	± [e]
298.15	-	0	75.6	0.2	1.395	54.2	0.3
298.15	1.05	0.247	43.0	0.2	1.384	31.1	0.2
298.15	2.01	0.401	28.32	0.06	1.373	20.6	0.1
298.15	3.10	0.509	17.83	0.04	1.361	13.10	0.07
298.15	4.00	0.600	13.39	0.03	1.351	9.92	0.05
298.15	5.01	0.663	9.84	0.03	1.339	7.35	0.04
298.15	7.14 [f]	0.817	7.02	0.01	1.325	5.30	0.03
298.15	10.13 [f]	0.858	5.50	0.01	1.317	4.18	0.02
298.15	6.43 [g]	1.0	0.057[h]	-	0.7105 [g]	0.0803 [g]	-
318.15	-	0	34.3	0.1	1.378	24.9	0.2
318.15	2.10	0.325	17.49	0.05	1.380	12.67	0.07
318.15	3.04	0.418	13.40	0.04	1.384	9.68	0.06
318.15	3.92	0.494	10.93	0.02	1.389	7.86	0.04
318.15	4.92	0.567	8.71	0.03	1.396	6.24	0.04
318.15	5.89	0.625	7.33	0.03	1.403	5.22	0.03
318.15	7.39	0.688	6.06	0.04	1.416	4.28	0.03
318.15	9.89	0.723	4.66	0.03	1.442	3.23	0.03
318.15	14.85	0.533	4.08	0.03	1.514	2.69	0.02
318.15	20.01	0.840	3.71	0.03	1.614	2.30	0.02
318.15	24.92	0.861	3.62	0.04	1.620	2.23	0.03
338.15	-	0	18.62	0.06	1.357	13.7	0.08
338.15	1.27	0.176	14.41	0.04	1.363	10.6	0.06
338.15	1.91	0.234	12.95	0.04	1.365	9.5	0.06
338.15	3.18	0.341	10.56	0.02	1.370	7.7	0.04
338.15	4.25	0.420	8.87	0.04	1.373	6.5	0.04
338.15	5.25	0.486	7.72	0.03	1.376	5.6	0.04
338.15	6.27	0.545	6.94	0.04	1.379	5.0	0.04
338.15	7.47	0.604	6.00	0.04	1.382	4.3	0.04
338.15	9.91	0.688	4.83	0.04	1.388	3.5	0.03
338.15	15.02	0.751	3.81	0.03	1.410	2.7	0.03

Standard Uncertainties: u(T)=0.1 K; u(p)=0.1MPa; u(ρ)=0.001g·cm^{-3}; u(η)=0.1mPa·s u(ν)=0.5 cSt. [a] Compositions were determined by interpolation of the VLE data of Ref. [34]. [b] standard deviation of 20 measurements; [c] interpolated from density data of Ref. [34]; [d] kinematic viscosity (ν) is defined as: $\nu = \frac{\eta}{\rho}$, where η is the dynamic viscosity and ρ is the mixture density ; [e] assumes a 5% error in the interpolated molar volume; [f] Vapor-Liquid-Liquid Equilibrium point: IL-rich phase viscosity; [g] properties of pure saturated liquid CO_2 from Ref. [49].

Table 5. Measured dynamic viscosity (η), interpolated density (ρ) and calculated kinematic viscosity (ν) of the $[C_6C_1Pyr][NTf_2]$ phase with pressure and composition of CO_2.

T (K)	p (MPa)	x_{CO2} [a]	η (mPa·s)	± [b]	ρ ($g \cdot cm^{-3}$) [c]	ν (cSt) [d]	± [e]
298.15	-	0	98.3	0.1	1.335	73.6	0.4
298.15	1.08	0.269	64.1	0.7	1.360	47.2	0.6
298.15	2.02	0.419	41.3	0.1	1.353	30.5	0.2
298.15	3.06	0.538	27.06	0.08	1.342	20.2	0.1
298.15	4.04	0.621	18.0	0.1	1.327	13.6	0.1
298.15	5.67	0.720	10.99	0.04	1.294	8.5	0.05
298.15	6.95 [f]	0.777	7.98	0.03	1.261	6.3	0.04
298.15	10.04 [f]	0.787	7.33	0.02	1.251	5.9	0.03
298.15	6.43 [g]	1.0	0.057 [g]	-	0.7105 [g]	0.0803 [g]	-
318.15	-	0	41.38	0.04	1.318	31.4	0.16
318.15	1.06	0.199	29.3	0.3	1.406	20.9	0.3
318.15	2.02	0.329	21.22	0.06	1.355	15.7	0.09
318.15	3.07	0.438	15.70	0.05	1.316	11.9	0.07
318.15	4.04	0.516	12.16	0.07	1.294	9.4	0.07
318.15	4.95	0.576	10.00	0.04	1.285	7.8	0.05
318.15	6.30	0.648	7.90	0.03	1.301	6.1	0.04
318.15	7.60	0.703	6.48	0.02	1.318	4.9	0.03
318.15	10.03	0.781	5.20	0.02	1.387	3.8	0.02
318.15	15.23	0.885	4.60	0.03	1.409	3.3	0.03
338.15	-	0	21.88	0.02	1.301	16.82	0.07
338.15	0.95	0.146	18.2	0.2	1.314	13.9	0.1
338.15	1.94	0.264	14.94	0.04	1.310	11.40	0.06
338.15	2.99	0.361	12.44	0.04	1.306	9.53	0.05
338.15	3.97	0.434	10.56	0.06	1.301	8.12	0.06
338.15	5.02	0.499	8.92	0.04	1.295	6.89	0.04
338.15	6.01	0.550	7.80	0.03	1.288	6.05	0.03
338.15	7.47	0.612	6.54	0.02	1.278	5.12	0.03
338.15	10.06	0.695	5.20	0.02	1.310	3.97	0.02
338.15	14.89	0.770	4.43	0.03	1.340	3.31	0.02

Standard Uncertainties: u(T)=0.1 K; u(p)=0.1MPa; u(ρ)=0.001g·cm^{-3}; u(η)=0.1mPa·s u(ν)=0.5 cSt. [a] Compositions were determined by interpolation of the VLE data of Ref. [34]. [b] standard deviation of 20 measurements; [c] interpolated from density data of Ref. [34]; [d] kinematic viscosity (ν) is defined as: $\nu = \frac{\eta}{\rho}$, where η is the dynamic viscosity and ρ is the mixture density ; [e] assumes a 5% error in the interpolated molar volume; [f] Vapor-Liquid-Liquid Equilibrium point: IL-rich phase viscosity; [g] properties of pure saturated liquid CO_2 from Ref. [49].

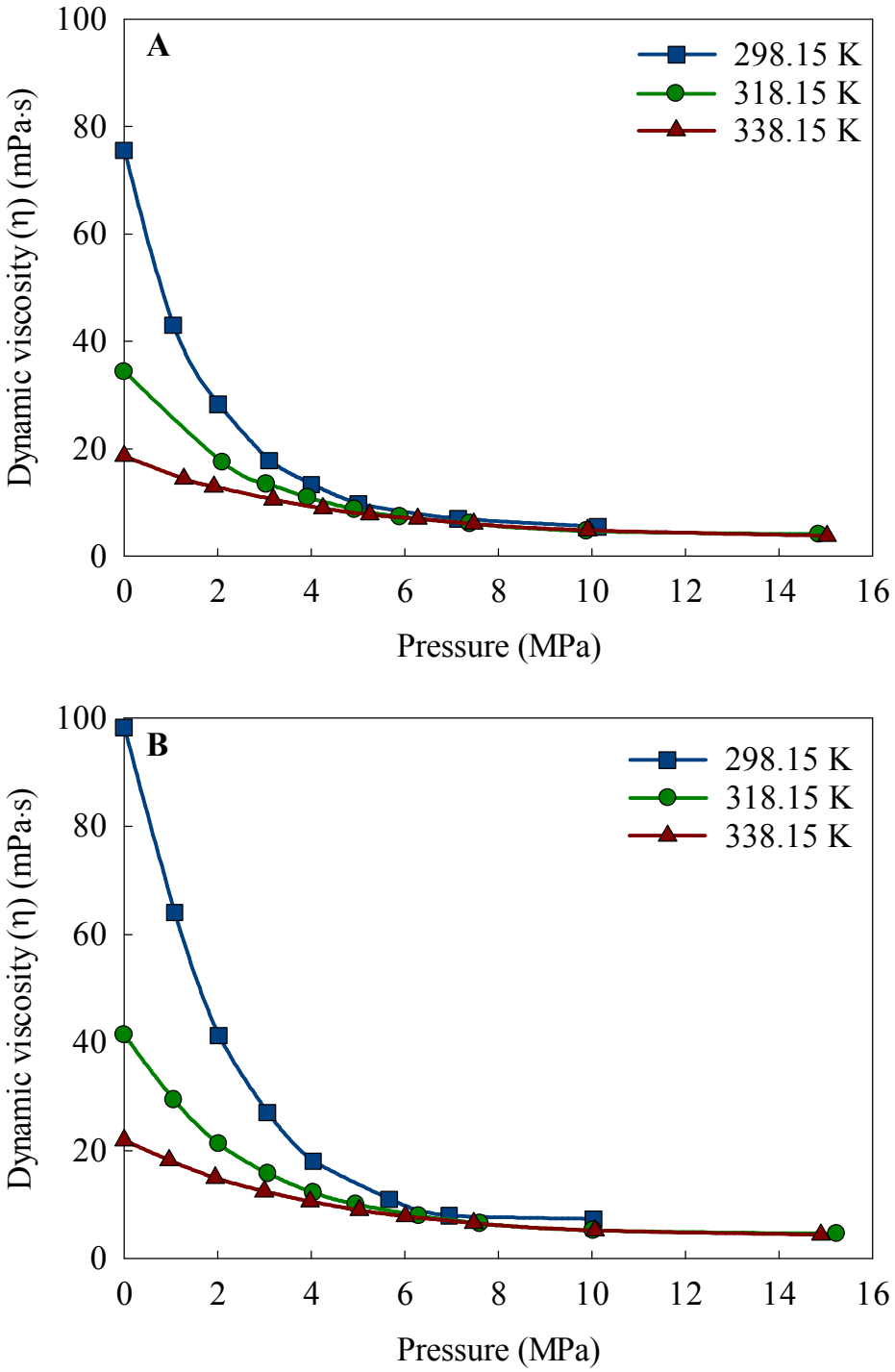

Figure 6. The viscosity of CO_2-saturated $[C_4C_1Pyr][NTf_2]$ (A) and $[C_6C_1Pyr][NTf_2]$ (B) as a function of CO_2 pressure at 298.15, 318.15 and 338.15 K isotherms (smoothed lines). The lowest pressure viscosity point is free of CO_2 at ambient pressure.

Interestingly, though the ambient pressure viscosity of $[C_6C_1Pyr][NTf_2]$ at 318.15 K is 98.3 mPa·s and of pure $[C_4C_1Pyr][NTf_2]$ is 75.6 mPa·s, their dynamic viscosity at similar CO_2

pressures of 6.95 MPa and 7.14 MPa are 7.98 and 7.0 mPa·s, respectively. This observation reveals that for a fixed temperature and certain CO_2 pressures, it is possible to achieve very similar dynamic viscosities for both ionic liquids, despite large differences in their pure dynamic viscosity values. In addition, under those high-pressure conditions, the alkyl-chain length of the ionic liquid cation has a small contribution to the viscosity differences among the ionic liquid/ CO_2 mixtures, as the CO_2 pressure (composition) is the major factor contributing to the observed viscosity reduction.

3.3. Comparison of $[C_nC_1Pyr][NTf_2]$ /CO_2 mixture viscosities

The viscosities measured for all the pyrrolidinium-based ionic liquids were compared and shown in Figure 7. Increasing the alkyl chain of the cation increases the ambient pressure viscosity, which is shown by comparing $[C_3C_1Pyr][NTf_2]$ with $[C_4C_1Pyr][NTf_2]$ and $[C_6C_1Pyr][NTf_2]$. For example, the viscosity of pure $[C_4C_1Pyr][NTf_2]$ is 30% higher than $[C_4C_1Pyr][NTf_2]$ at ambient pressure. In contrast, the viscosity of $[C_4C_1Pyr][NTf_2]$ is only 8% higher $[C_3C_1Pyr][NTf_2]$ at 10 MPa of CO_2 pressure. A similar trend has been found for imidazolium- and pyridinium-based ionic liquids.[30, 51-53] For instance, Ahosseini *et al.* reported that $[C_{10}C_1im][NTf_2]$ is 216% more viscous than $[C_2C_1im][NTf_2]$ at 298.15 K.[25, 54-56] However, the viscosity of all these ionic liquids becomes very similar at the same at higher CO_2 pressures. Unfortunately, the authors are aware of no known literature data for the viscosity of pyrrolidinium-based molten salts under CO_2 pressure for comparison.

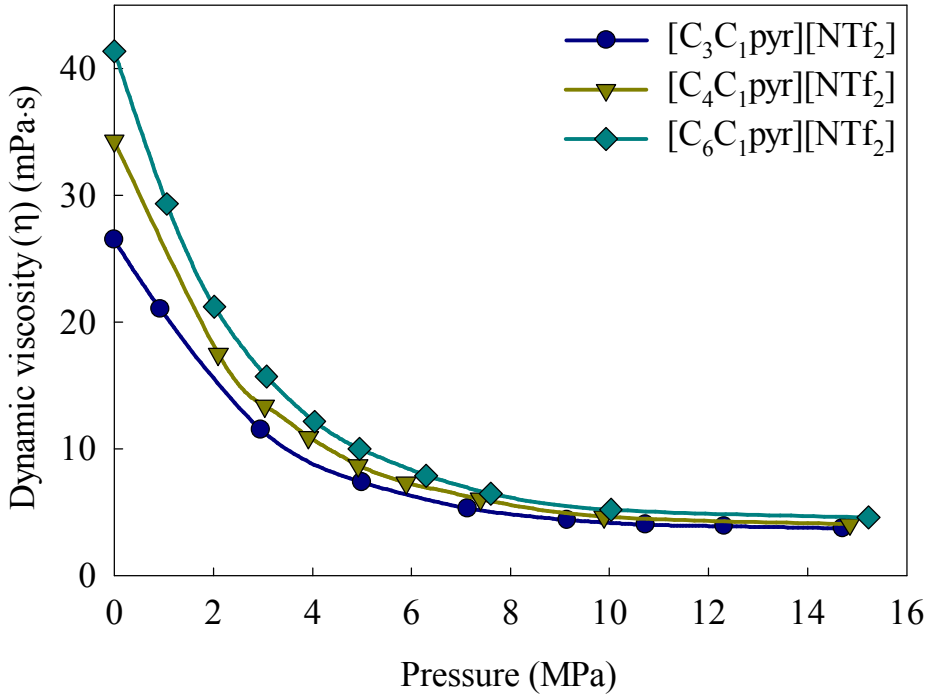

Figure 7. Comparison of CO_2-saturated $[C_nC_1Pyr][NTf_2]$ viscosities at 318.15 K isotherm (smoothed lines). The lowest pressure viscosity point is free of CO_2 at ambient pressure.

3.4. Correlation of viscosity with diffusivity for $[C_nC_1im][NTf_2]$ /CO_2 mixture

We have recently determined the Fickian diffusivity (D_{12}) of CO_2 in the $[C_3C_1Pyr][NTf_2]$, $[C_4C_1Pyr][NTf_2]$ and $[C_6C_1Pyr][NTf_2]$ ionic liquids at CO_2 pressures up to 2 MPa and at 298.15 and 318.15 K isotherms.[34] The diffusivity and viscosity of $[C_nC_1Pyr][NTf_2]$/ CO_2 mixture at given temperature and CO_2 pressure (composition) are depicted in

Ionic Liquid	*P* (MPa)	T (K)					
		298.15			318.15		
		x_{CO2} [a]	η (mPa·s) [b]	D (10^{-10} m^2/s)	x_{CO2} [a]	η (mPa·s) [b]	D (10^{-10} m^2/s)
$[C_3C_1Pyr][NTf_2]$	0.1	0.026	55.0	1.3 ± 0.1	0.025	26.5	2.7 ± 0.1
	1	0.234	41.1	1.8 ± 0.3	0.182	20.6	3.0 ± 0.3
	2	0.395	27.3	2.4 ± 0.4	0.309	15.3	3.7 ± 0.8

$[C_4C_1Pyr][NTf_2]$	0.1	0.030	71.5	1.3 ± 0.1	0.020	34.3	2.2 ± 0.1
	1	0.240	43.0	1.6 ± 0.2	0.177	25.4	2.9 ± 0.3
	2	0.415	28.3	3.0 ± 0.9	0.312	18.0	3.3 ± 0.7
$[C_6C_1Pyr][NTf_2]$	0.1	0.029	94.4	1.6 ± 0.1	0.027	41.4	2.3 ± 0.1
	1	0.251	64.1	2.4 ± 0.3	0.195	29.3	3.8 ± 0.4
	2	0.419	41.3	4 ± 1	0.333	21.2	3.8 ± 0.7 [c]

Table 6. As expected, the diffusivity of CO_2 in $[C_nC_1Pyr][NTf_2]$ ionic liquids is inversely proportional to $[C_nC_1Pyr][NTf_2]/CO_2$ mixture viscosities, according to the Stokes-Einstein equation. For instance, the diffusivity of $[C_3C_1Pyr][NTf_2]/CO_2$ mixture at 298.15 K increased about 85% with increasing CO_2 pressure from 0.1 to 20 MPa (3 to 40 mol% CO_2 composition), due to a viscosity decrease approximately of 50 %. It is most striking for $[C_6C_1Pyr][NTf_2]$ which has 2.5-fold improvement in diffusivity (with a 56% reduction in viscosity) with increasing CO_2 pressure from 0.1 to 2 MPa (3 to 41 mol% CO_2 composition) at 298.15 K. At 318.15 K and similar increasing CO_2 pressures, the diffusivity enhancement of $[C_3C_1Pyr][NTf_2]/CO_2$ was about 37 %, while for $[C_6C_1Pyr][NTf_2]/CO_2$ a 65% improvement in the diffusivity was found. Similar qualitative trends in diffusivity with gas solubility and viscosity were observed by Ahosseini *et al.* for the system of 1,1,1,2-tetrafluoroethane in the IL, 1-hexyl-3-methyl-imidazolium bis(trifluoromethylsulfonyl)amide ($[C_6C_1im][NTf_2]$); albeit with self-diffusivity of the gas and IL.[57]

Ionic Liquid	***P*** **(MPa)**	**T (K)**					
		298.15			**318.15**		
		x_{CO2} [a]	η **(mPa·s)** [b]	***D*** **(10^{-10} m^2/s)**	x_{CO2} [a]	η **(mPa·s)** [b]	***D*** **(10^{-10} m^2/s)**
$[C_3C_1Pyr][NTf_2]$	0.1	0.026	55.0	1.3 ± 0.1	0.025	26.5	2.7 ± 0.1
	1	0.234	41.1	1.8 ± 0.3	0.182	20.6	3.0 ± 0.3
	2	0.395	27.3	2.4 ± 0.4	0.309	15.3	3.7 ± 0.8
$[C_4C_1Pyr][NTf_2]$	0.1	0.030	71.5	1.3 ± 0.1	0.020	34.3	2.2 ± 0.1
	1	0.240	43.0	1.6 ± 0.2	0.177	25.4	2.9 ± 0.3
	2	0.415	28.3	3.0 ± 0.9	0.312	18.0	3.3 ± 0.7
$[C_6C_1Pyr][NTf_2]$	0.1	0.029	94.4	1.6 ± 0.1	0.027	41.4	2.3 ± 0.1
	1	0.251	64.1	2.4 ± 0.3	0.195	29.3	3.8 ± 0.4

2	0.419	41.3	4 ± 1	0.333	21.2	3.8 ± 0.7 [c]

Table 6. Diffusivity and viscosity $[C_nC_1Pyr][NTf_2]$/ CO_2 mixtures at varying temperatures, and CO_2 pressures (and CO_2 compositions).

Standard Uncertainties: u(T)=0.1K; u(P)=0.1 MPa; u(ρ)=0.5 mPa.S; u(D)=~50%. [a] Compositions were determined by interpolation of the VLE data of Ref. [34]; [b] Interpolated from mixture viscosity data shown in Tables 4-5. [c] CO_2 pressure of 1.8 MPa.

These diffusivity data may be analyzed with the current mixture viscosity data starting from the Stokes-Einstein theory.

$$\frac{D}{T} = \frac{A}{\eta} \qquad \text{Equation 1}$$

where A is a constant that is a function of the Boltzmann constant, shape parameter, and hydrodynamic radius. As such, diffusivity divided by absolute temperature is inversely proportional to the viscosity of the mixture assuming the shape factor and hydrodynamic radius do not change with CO_2 composition, *i.e.* A is a constant. Figure 8 illustrates the diffusivity divided by the absolute temperature versus the mixture viscosity interpolated from the data taken in this study. A good correlation between the different temperatures for each binary system are observed. In addition, the data between the $[C_3C_1Pyr]$ and $[C_4C_1Pyr][NTf_2]$ ILs are very well correlated by Stokes-Einstein theory. The A values (Equation 1) (and R^2) are 4.93 (0.90), 4.32 (0.80), and 2.7 (0.49) for $[C_3C_1Pyr]$, $[C_4C_1Pyr][NTf_2]$, and $[C_6C_1Pyr][NTf_2]$ respectively. As these two ILs are only structurally different by 1 methylene group (-CH_2), one would assume that they share a similar hydrodynamic radius. The $[C_6C_1Pyr][NTf_2]$ IL has a much longer alkyl chain and presumably would have a larger radius and thus a different slope as observed in Figure 8.

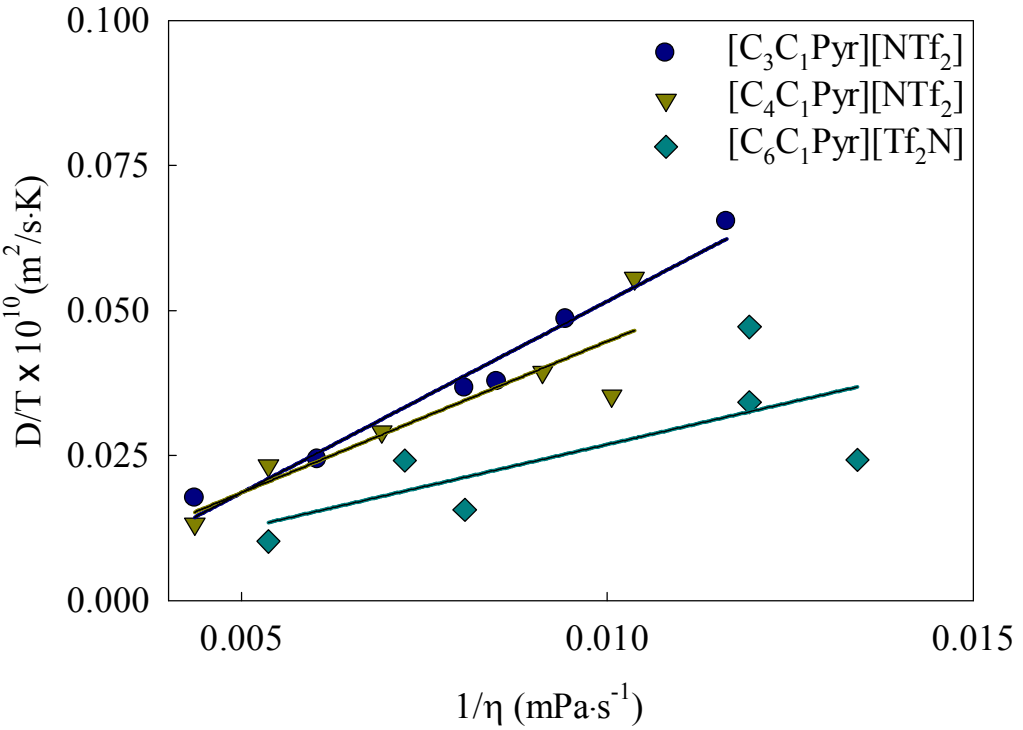

Figure 8. Fickian diffusivity divided by temperature as function of the inverse of $[C_nC_1Pyr][NTf_2]/CO_2$ mixture viscosity for each $[C_3C_1Pyr][NTf_2]$, $[C_4C_1Pyr][NTf_2]$ and $[C_6C_1Pyr][NTf_2]$ studied at 298.15 K and 318.15 K.

4. Conclusions

The present work reports the experimental liquid viscosities for a selection of 1-alkyl-1-methyl-pyrrolidinium bis(trifluoromethylsulfonyl)imide ionic liquids, $[C_3C_1Pyr][NTf_2]$, $[C_4C_1Pyr][NTf_2]$, and $[C_6C_1Pyr][NTf_2]$, saturated with CO_2 at 298.15, 318.15, and 338.15 K and CO_2 pressures up to 25 MPa. In the temperature range investigated herein, the viscosity of the liquid-phase dramatically decreases with increasing of CO_2 pressure but the decrease becomes less significant at higher CO_2 pressures. At lower CO_2 pressures, the temperature has a higher impact on the solubility of CO_2 in the ionic liquid, thus the viscosity reduction is more significant for lower temperatures. In contrast, at higher pressures, the CO_2 composition in ionic liquid only marginally increases with pressure, and, thus, only a small decrease in the mixture viscosity is observed. The influence of alkyl-chain length in the pyrrolidinium cation

with [NTf_2] anion changed the quantitative viscosity behavior with pressure. While the ambient pressure viscosity of the pure ionic liquids increased in the order [C_3C_1Pyr][NTf_2] < [C_4C_1Pyr][NTf_2] < [C_6C_1Pyr][NTf_2], the relative change in viscosity as a function of CO_2 mole fraction is similar at a given temperature. Moreover, at high CO_2 compositions, the mixture viscosity was similar for all of the ILs studied despite the large differences in their pure IL viscosity. In addition, the diffusivity of CO2 into these ILs is inversely proportional to the mixture viscosities measured here confirming an approximate Stokes-Einstein relationship. This study indicates that applications with ionic liquids, such as reactions and separations, will potentially achieve better performance in a system with compressed CO_2 over the pure ionic liquid itself.

5. Acknowledgements

Work supported through the INL Laboratory Directed Research & Development (LDRD) Program under DOE Idaho Operations Office Contract DE-AC07-05ID14517.

6. Funding

Funding to the University of Kansas was provided through subcontract #195234 from Idaho National Laboratory.

7. References

1. Holbrey, J. D.; Seddon, K. R., Ionic Liquids. *Clean Prod. Proc.* **1999,** 1, 223-236.
2. Fillion, J. J.; Xia, H.; Desilva, M. A.; Quiroz-Guzman, M.; Brennecke, J. F., Phase Transitions, Decomposition Temperatures, Viscosities, and Densities of Phosphonium, Ammonium, and Imidazolium Ionic Liquids with Aprotic Heterocyclic Anions. *J. Chem. Eng. Data* **2016,** 61, 2897-2914.
3. Fredlake, C. P.; Crosthwaite, J. M.; Hert, D. G.; Aki, S. N. V. K.; Brennecke, J. F., Thermophysical properties of imidazolium-based ionic liquids. *J. Chem. Eng. Data* **2004,** 49, 954-964.
4. Huddleston, J. G.; Rogers, R. D., Room temperature ionic liquids as novel media for 'clean'liquid–liquid extraction. *Chem. Comm.* **1998**, 1765-1766.
5. Karpinska, M.; Wlazlo, M.; Zawadzki, M.; Domanska, U., Liquid-liquid separation of hexane/hex-1-ene and cyclohexane/cyclohexene by dicyanamide-based ionic liquids. *J. Chem. Thermodyn.* **2018,** 116, 299-308.
6. Quinn, B. M.; Ding, Z. F.; Moulton, R.; Bard, A. J., Novel electrochemical studies of ionic liquids. *Langmuir* **2002,** 18, 1734-1742.
7. Azaceta, E.; Lutz, L.; Grimaud, A.; Vicent-Luna, J. M.; Hamad, S.; Yate, L.; Cabanero, G.; Grande, H. J.; Anta, J. A.; Tarascon, J. M.; Tena-Zaera, R., Electrochemical Reduction of Oxygen in Aprotic Ionic Liquids Containing Metal Cations: A Case Study on the Na-O_2 system. *ChemSusChem* **2017,** 10, 1616-1623.
8. Al-Masri, D.; Yunis, R.; Hollenkamp, A. F.; Pringle, J. M., A symmetrical ionic liquid/Li salt system for rapid ion transport and stable lithium electrochemistry. *Chem. Comm.* **2018,** 54, 3660-3663.
9. Dupont, J.; de Souza, R. F.; Suarez, P. A. Z., Ionic liquid (molten salt) phase organometallic catalysis. *Chem. Rev.* **2002,** 102, 3667-3691.
10. Wasserscheid, P.; Keim, W., Ionic liquids—new "solutions" for transition metal catalysis. *Angew. Chem. Intl. Ed.* **2000,** 39, 3772-3789.
11. Dhakshinamoorthy, A.; Asiri, A. M.; Alvaro, M.; Garcia, H., Metal organic frameworks as catalysts in solvent-free or ionic liquid assisted conditions. *Green Chem.* **2018,** 20, 86-107.
12. Cull, S.; Holbrey, J.; Vargas□Mora, V.; Seddon, K.; Lye, G., Room□temperature ionic liquids as replacements for organic solvents in multiphase bioprocess operations. *Biotech. Bioeng.* **2000,** 69, 227-233.

13. Itoh, T., Ionic Liquids as Tool to Improve Enzymatic Organic Synthesis. *Chem. Rev.* **2017,** 117, 10567-10607.

14. Zhang, L.; Chen, J.; Lv, J. X.; Wang, S. F.; Cui, Y., Progress and Development of Capture for CO_2 by Ionic Liquids. *Asian J Chem* **2013,** 25, 2355-2358.

15. Nikolaeva, D.; Azcune, I.; Sheridan, E.; Sandru, M.; Genua, A.; Tanczyk, M.; Jaschik, M.; Warmuzinski, K.; Jansen, J. C.; Vankelecom, I. F. J., Poly(vinylbenzyl chloride)-based poly(ionic liquids) as membranes for CO_2 capture from flue gas. *J Mater Chem A* **2017,** 5, 19808-19818.

16. Ahosseini, A.; Ren, W.; Scurto, A. M., Understanding Biphasic Ionic Liquid/CO2 Systems for Homogeneous Catalysis: Hydroformylation. *Ind Eng Chem Res* **2009,** 48, 4254-4265.

17. Solinas, M.; Pfaltz, A.; Cozzi, P. G.; Leitner, W., Enantioselective hydrogenation of imines in ionic liquid/carbon dioxide media. *J. Am. Chem. Soc.* **2004,** 126, 16142-16147.

18. Shiflett, M. B.; Yokozeki, A., Phase Behavior of Carbon Dioxide in Ionic Liquids: [emim][Acetate], [emim][Trifluoroacetate], and [emim][Acetate] plus [emim][Trifluoroacetate] Mixtures. *J. Chem. Eng. Data* **2009,** 54, 108-114.

19. Kamps, A. P. S.; Tuma, D.; Xia, J. Z.; Maurer, G., Solubility of CO_2 in the ionic liquid [bmim][PF_6]. *J. Chem. Eng. Data* **2003,** 48, 746-749.

20. Shiflett, M. B.; Yokozeki, A., Solubility of CO_2 in room temperature ionic liquid [hmim][Tf_2N]. *J. Phys. Chem. B* **2007,** 111, 2070-2074.

21. Klahn, M.; Seduraman, A., What Determines CO_2 Solubility in Ionic Liquids? A Molecular Simulation Study. *J. Phys. Chem. B* **2015,** 119, 10066-10078.

22. Carvalho, P. J.; Kurnia, K. A.; Coutinho, J. A. P., Dispelling some myths about the CO_2 solubility in ionic liquids. *Phys Chem Chem Phys* **2016,** 18, 14757-14771.

23. Nunes da Ponte, M.; Zakrzewska, M. E., Volumetric and phase behaviour of mixtures of fluoroalkylphosphate-based ionic liquids with high pressure carbon dioxide. *J. Supercrit. Fluid.* **2016,** 113, 61-65.

24. Yadav, A.; Guha, A.; Pandey, A.; Pal, M.; Trivedi, S.; Pandey, S., Densities and dynamic viscosities of ionic liquids having 1-butyl-3-methylimidazolium cation with different anions and bis(trifluoromethylsulfonyl)imide anion with different cations in the temperature range (283.15 to 363.15)K. *J. Chem. Thermodyn.* **2018,** 116, 67-75.

25. Ahosseini, A.; Scurto, A. M., Viscosity of Imidazolium-Based Ionic Liquids at Elevated Pressures: Cation and Anion Effects. *Int. J. Thermophys.* **2008,** 29, 1222-1243.

26. Lu, J.; Liotta, C. L.; Eckert, C. A., Spectroscopically probing microscopic solvent properties of room-temperature ionic liquids with the addition of carbon dioxide. *J. Phys. Chem. A* **2003,** 107, 3995-4000.

27. Liu, Z. M.; Wu, W. Z.; Han, B. X.; Dong, Z. X.; Zhao, G. Y.; Wang, J. Q.; Jiang, T.; Yang, G. Y., Study on the phase behaviors, viscosities, and thermodynamic properties of CO_2/[C_4mim][PF_6]/methanol system at elevated pressures. *Chem. Eur. J.* **2003,** 9, 3897-3903.

28. Tomida, D.; Kumagai, A.; Qiao, K.; Yokoyama, C., Viscosity of 1-butyl-3-methylimidazolium hexafluorophosphate plus CO_2 mixture. *J. Chem. Eng. Data* **2007,** 52, 1638-1640.

29. Tomida, D.; Kumagai, A.; Qiao, K.; Yokoyama, C., Viscosity of 1-butyl-3-methylimidazolium tetrafluoroborate + CO_2 mixture. *High Temp. High Press.* **2008,** 37, 81-89.

30. Ahosseini, A.; Ortega, E.; Sensenich, B.; Scurto, A. M., Viscosity of n-alkyl-3-methyl-imidazolium bis(trifluoromethylsulfonyl)amide ionic liquids saturated with compressed CO_2. *Fluid Phase Equil.* **2009,** 286, 62-68.

31. Lopes, J. M.; Kareth, S.; Bermejo, M. D.; Martin, A.; Weidner, E.; Cocero, M. J., Experimental determination of viscosities and densities of mixtures carbon dioxide + 1-allyl-3-methylimidazolium chloride. Viscosity correlation. *J. Supercrit. Fluids* **2016,** 111, 91-96.

32. Iguchi, M.; Kasuya, K.; Sato, Y.; Aida, T. M.; Watanabe, M.; Smith, R. L., Jr., Viscosity reduction of cellulose + 1-butyl-3-methylimidazolium acetate in the presence of CO_2. *Cellulose* **2013,** 20, 1353-1367.

33. Goodrich, B. F.; de la Fuente, J. C.; Gurkan, B. E.; Zadigian, D. J.; Price, E. A.; Huang, Y.; Brennecke, J. F., Experimental Measurements of Amine-Functionalized Anion-Tethered Ionic Liquids with Carbon Dioxide. *Ind. Eng. Chem. Res.* **2011,** 50, 111-118.

34. Turnaoglu, T.; Minnick, D. L.; Colaco Morais, A. R.; Scurto, A. M.; Shiflett, M. B.; Baek, D. L.; Fox, R. V., Vapor-Liquid Equilibrium of 1-n-Alkyl-1-Methyl Pyrrolidinium bis(trifluoromethylsulfonyl)amide Ionic Liquids and Compressed CO_2 *Accepted J. Chem. Eng. Data* **2019**.

35. Duncan, A. M.; Ahosseini, A.; McHenry, R.; Depcik, C. D.; Stagg-Williams, S. M.; Scurto, A. M., High-Pressure Viscosity of Biodiesel from Soybean, Canola, and Coconut Oils. *Energy & Fuels* **2010,** 24, 5708-5716.

36. Jin, H.; O'Hare, B.; Dong, J.; Arzhantsev, S.; Baker, G. A.; Wishart, J. F.; Benesi, A. J.; Maroncelli, M., Physical properties of ionic liquids consisting of the 1-butyl-3-

methylimidazolium cation with various anions and the bis(trifluoromethylsulfonyl)imide anion with various cations. *J. Phys. Chem. B* **2008,** 112, 81-92.

37. Vranes, M.; Dozic, S.; Djeric, V.; Gadzuric, S., Physicochemical Characterization of 1-Butyl-3-methylimidazolium and 1-Butyl-1-methylpyrrolidinium Bis(trifluoromethylsulfonyl)imide. *J. Chem. Eng. Data* **2012,** 57, 1072-1077.

38. Gacino, F. M.; Regueira, T.; Lugo, L.; Comunas, M. J. P.; Fernandez, J., Influence of Molecular Structure on Densities and Viscosities of Several Ionic Liquids. *J Chem Eng Data* **2011,** 56, 4984-4999.

39. Harris, K. R.; Woolf, L. A., Transport Properties of N-Butyl-N-methylpyrrolidinium Bis(trifluoromethylsulfonyl)amide. *J Chem Eng Data* **2011,** 56, 4672-4685.

40. Gonzalez, B.; Gonzalez, E. J., Physical properties of the pure 1-methyl-1-propylpyrrolidinium bis(trifluoromethylsulfonyl) imide ionic liquid and its binary mixtures with alcohols. *J Chem Thermodyn* **2014,** 68, 109-116.

41. MacFarlane, D. R.; Meakin, P.; Sun, J.; Amini, N.; Forsyth, M., Pyrrolidinium imides: A new family of molten salts and conductive plastic crystal phases. *J. Phys. Chem. B* **1999,** 103, 4164-4170.

42. Makino, T.; Kanakubo, M.; Umecky, T.; Suzuki, A.; Nishida, T.; Takano, J., Pressure-volume-temperature-composition relations for carbon dioxide plus pyrrolidinium-based ionic liquid binary systems. *Fluid Phase Equil.* **2013,** 360, 253-259.

43. Lide, D. R., *CRC Handbook of Chemistry and Physics*. 73nd ed.; Press, Boca Raton: 1992.

44. Rodrigues, A. S. M. C.; Almeida, H. F. D.; Freire, M. G.; Lopes-da-Silva, J. A.; Coutinho, J. A. P.; Santos, L. M. N. B. F., The effect of n vs. iso isomerization on the thermophysical properties of aromatic and non-aromatic ionic liquids. *Fluid Phase Equilibr* **2016,** 423, 190-202.

45. Seoane, R. G.; Corderi, S.; Gomez, E.; Calvar, N.; Gonzalez, E. J.; Macedo, E. A.; Dominguez, A., Temperature Dependence and Structural Influence on the Thermophysical Properties of Eleven Commercial Ionic Liquids. *Ind. Eng. Chem. Res* **2012,** 51, 2492-2504.

46. Pereiro, A. B.; Veiga, H. I. M.; Esperanca, J. M. S. S.; Rodriguez, A., Effect of temperature on the physical properties of two ionic liquids. *J. Chem. Thermodyn.* **2009,** 41, 1419-1423.

47. Hiraga, Y.; Hagiwara, S.; Sato, Y.; Smith, R. L., Measurement and Correlation of High-Pressure Densities and Atmospheric Viscosities of Ionic Liquids: 1-Butyl-1-methylpyrrolidiniunn Bis(trifluoromethylsulfonyl)imide), 1-Allyl-3-methylimidazolium

Bis(trifluoromethylsulfonyl)imide, 1-Ethyl-3-methylimidazolium Tetracyanoborate, and 1-Hexyl-3-methylimidazolium Tetracyanoborate. *J. Chem. Eng. Data* **2018,** 63, 972-980.

48. Lu, J.; Liotta, C. L.; Eckert, C. A., Spectroscopically Probing Microscopic Solvent Properties of Room-Temperature Ionic Liquids with the Addition of Carbon Dioxide. *J. Phys. Chem. A* **2003,** 107, 3995.

49. Lemmon, E. W.; Huber, M. L.; McLinden, M. O. *NIST Reference Fluid Thermodynamic and Transport Properties - REFPROP Version 8.0*, Gaithersburg, Maryland, 2007.

50. Blanchard, L. A.; Gu, Z. Y.; Brennecke, J. F., High-pressure phase behavior of ionic liquid/CO_2 systems. *J. Phys. Chem. B* **2001,** 105, 2437-2444.

51. Abbott, A. P., Application of hole theory to the viscosity of ionic and molecular liquids. *ChemPhysChem* **2004,** 5, 1242-1246.

52. Bonhote, P.; Dias, A. P.; Papageorgiou, N.; Kalyanasundaram, K.; Gratzel, M., Hydrophobic, highly conductive ambient-temperature molten salts. *Inorg. Chem.* **1996,** 35, 1168-1178.

53. Crosthwaite, J. M.; Muldoon, M. J.; Dixon, J. K.; Anderson, J. L.; Brennecke, J. F., Phase transition and decomposition temperatures, heat capacities and viscosities of pyridinium ionic liquids. *J. Chem. Thermodyn.* **2005,** 37, 559-568.

54. Rogers, R. D.; Seddon, K. R., Ionic liquids - Solvents of the future? *Science* **2003,** 302, 792-793.

55. Ficke, L. E.; Brennecke, J. F., Interactions of Ionic Liquids and Water. *J. Phys. Chem. B* **2010,** 114, 10496-10501.

56. Welton, T., Room-temperature ionic liquids. Solvents for synthesis and catalysis. *Chem. Rev.* **1999,** 99, 2071-2083.

57. Ahosseini, A.; Ren, W.; Weatherley, L. R.; Scurto, A. M., Viscosity and self-diffusivity of ionic liquids with compressed hydrofluorocarbons: 1-Hexyl-3-methyl-imidazolium bis(trifluoromethylsulfonyl)amide and 1,1,1,2-tetrafluoroethane. *Fluid Phase Equil.* **2017,** 437, 34-42.

List of Tables:

Table 3. Measured dynamic viscosity (η), interpolated density (ρ) and calculated kinematic viscosity (ν) of the [C3C1Pyr][NTf2] phase with respect to CO2 pressure and composition.

Table 4. Measured dynamic viscosity (η), interpolated density (ρ) and calculated kinematic viscosity (ν) of the [C4C1Pyr][NTf2] phase with pressure and composition of CO_2.

Table 5. Measured dynamic viscosity (η), interpolated density (ρ) and calculated kinematic viscosity (ν) of the [C6C1Pyr][NTf2] phase with pressure and composition of CO_2.

Table 6. Diffusivity and viscosity $[C_nC_1Pyr][NTf_2]$/ CO_2 mixtures at varying temperatures, and CO_2 pressures (and CO_2 compositions).

Ionic Liquid	***P*** **(MPa)**	**T (K)**					
		298.15			**318.15**		
		x_{CO2} [a]	***η*** **(mPa·s)** [b]	***D*** **(10^{-10} m^2/s)**	x_{CO2} [a]	***η*** **(mPa·s)** [b]	***D*** **(10^{-10} m^2/s)**
$[C_3C_1Pyr][NTf_2]$	0.1	0.026	55.0	1.3 ± 0.1	0.025	26.5	2.7 ± 0.1
	1	0.234	41.1	1.8 ± 0.3	0.182	20.6	3.0 ± 0.3
	2	0.395	27.3	2.4 ± 0.4	0.309	15.3	3.7 ± 0.8
$[C_4C_1Pyr][NTf_2]$	0.1	0.030	71.5	1.3 ± 0.1	0.020	34.3	2.2 ± 0.1
	1	0.240	43.0	1.6 ± 0.2	0.177	25.4	2.9 ± 0.3
	2	0.415	28.3	3.0 ± 0.9	0.312	18.0	3.3 ± 0.7
$[C_6C_1Pyr][NTf_2]$	0.1	0.029	94.4	1.6 ± 0.1	0.027	41.4	2.3 ± 0.1
	1	0.251	64.1	2.4 ± 0.3	0.195	29.3	3.8 ± 0.4
	2	0.419	41.3	4 ± 1	0.333	21.2	3.8 ± 0.7 [c]

List of Figures:

Figure 1. Chemical structures of the 1-n-alkyl-1-methyl-pyrrolidinium bis(trifluoromethylsulfonyl)imide ionic liquids investigated in the present work.

Figure 2. Effect of CO2 pressure on liquid viscosity and on mole fraction concentration of CO2 in [C3C1Pyr][NTf2] at 318.15 K (smoothed lines). Solubility data is interpolated from Ref. 34. The lowest pressure viscosity point is free of CO2 at ambient pressure.

Figure 3. The viscosity of CO2-saturated [C3C1Pyr][NTf2] as a function of CO2 pressure (A) and mole fraction concentration of CO2 in the liquid phase (B) at 298.15, 318.15 and 338.15 K isotherms (smoothed lines). The lowest pressure/ composition viscosity point is free of CO2 at ambient pressure.

Figure 4. Normalized viscosity to the ambient pressure viscosity of pure [C3C1Pyr][NTf2] as function of CO2 composition at 298.15, 318.15 and 338.15 K isotherms (smoothed lines). The lowest composition/ viscosity point is free of CO2 at ambient pressure.

Figure 5. Kinematic viscosity (ν) of [C3C1Pyr][NTf2] as function of CO2 composition at 298.15, 318.15 and 338.15 K isotherms (smoothed lines). The lowest composition viscosity point is free of CO2 at ambient pressure.

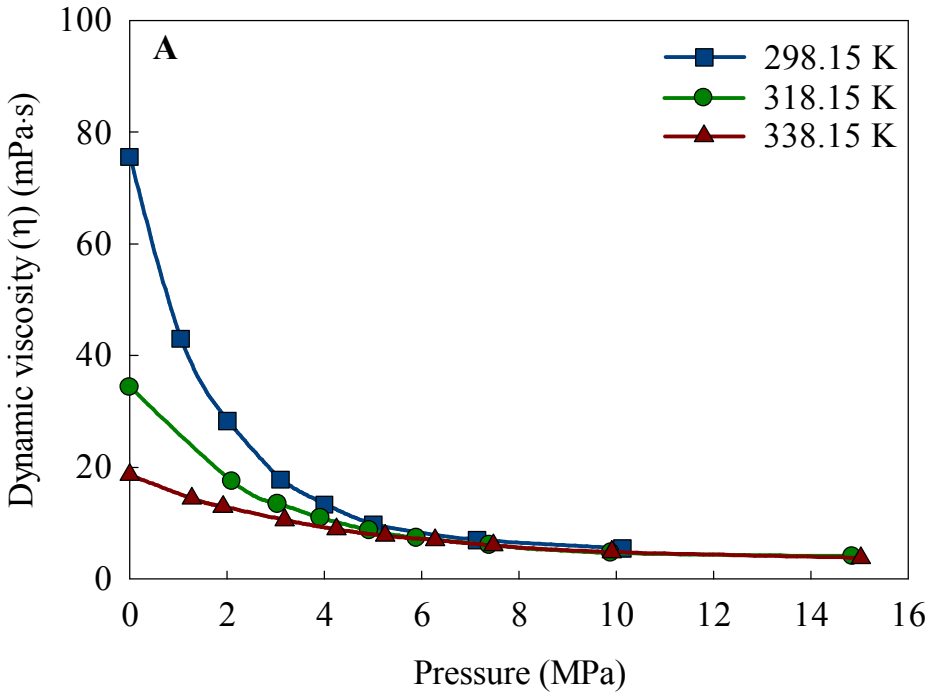

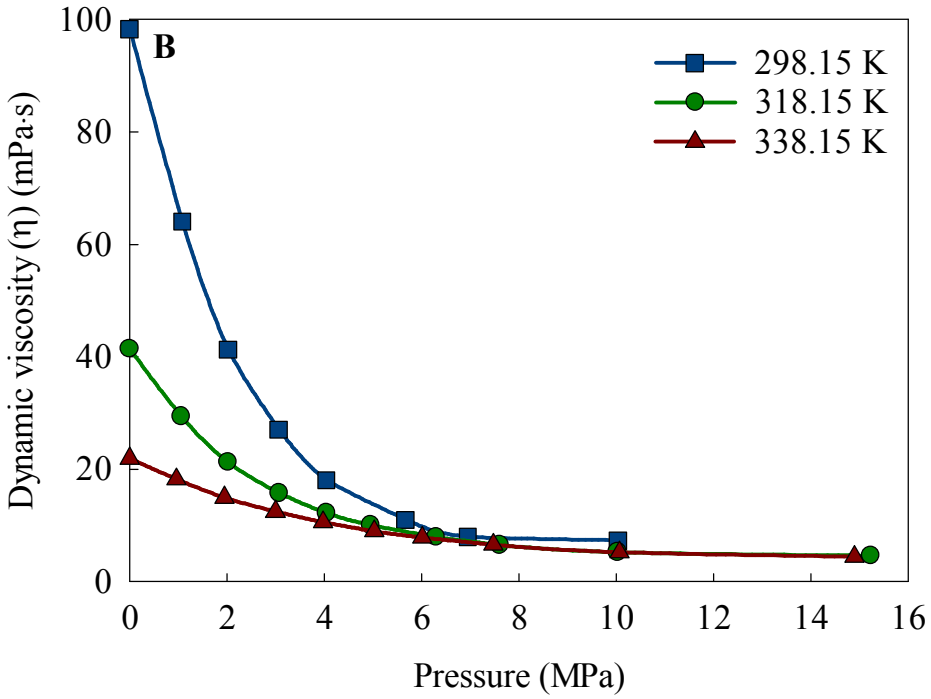

Figure 6. The viscosity of CO2-saturated [C4C1Pyr][NTf2] (A) and [C6C1Pyr][NTf2] (B) as a function of CO2 pressure at 298.15, 318.15 and 338.15 K isotherms (smoothed lines). The lowest pressure viscosity point is free of CO2 at ambient pressure.

Figure 7. Comparison of CO2-saturated [CnC1Pyr][NTf2] viscosities at 318.15 K isotherm (smoothed lines). The lowest pressure viscosity point is free of CO2 at ambient pressure.

Figure 8. Fickian diffusivity divided by temperature as function of the inverse of [CnC1Pyr][NTf2]/CO2 mixture viscosity for each [C3C1Pyr][NTf2], [C4C1Pyr][NTf2] and [C6C1Pyr][NTf2] studied at 298.15 K and 318.15 K.